



# Photoelectrocatalytic degradation of aniline over rutile TiO<sub>2</sub>/Ti electrode thermally formed at 600 °C

W.H. Leng\*, Z. Zhang, J.Q. Zhang

*Department of Chemistry, Zhejiang University, Yuquan District, Hangzhou 310027, China*

Received 5 January 2003; accepted 14 April 2003

## Abstract

The photoelectrochemical oxidation of aniline on rutile form TiO<sub>2</sub> film electrodes prepared by direct thermal oxidation of titanium sheet was studied both in single and double compartment photoreactor. The results showed that the rutile form of TiO<sub>2</sub>/Ti electrode had excellent photoactivity by applying anodic bias potential and irradiation simultaneously. Oxygen and its reduction products could accelerate the oxidation rate of aniline though its supply was not necessary in this system. The oxidation rate of aniline performed in single compartment cell was larger than that in double compartment cell under the conditions of either by nitrogen or air purging. The oxidation rate could be evaluated by the photocurrent, but it was dependent on the presence of oxygen. The photocurrent efficiency for aniline degradation was related to potential, pH, and single/double compartment cell. Total mineralization of aniline requires a much longer illumination time than its disappearance.

© 2003 Elsevier B.V. All rights reserved.

*Keywords:* Titanium dioxide; Photoanode; Aniline; Photoelectrocatalysis; Thermally oxidation

## 1. Introduction

Over the last few decades, there has been a growing interest in the application of photocatalysis towards the treatment of polluted water [1–5]. Since it needs to separate the spent catalyst particles for the slurry system, a great of reports have been dealt with the use of supported photocatalysts, especially those are immobilized over an electrically conducting substrates due to by which it can improve the efficiency of organics degradation through imposing an anodic bias potential [2–11]. Among the photocatalysts, TiO<sub>2</sub> is the most attractive one for purifying and treating of water. The most published work to date has dealt with the use of anatase form of TiO<sub>2</sub> electrode [2–9] and the ru-

tile TiO<sub>2</sub> photoelectrode has seldom been investigated [10,11], which may be attributed to its low specific surface area, poor adsorption for oxygen and low photoactivity in photocatalytic reaction [1,10]. However, the rutile TiO<sub>2</sub> photocatalyst may often be encountered, e.g. the popular photocatalyst, Degussa P-25, contains ca. 30% rutile TiO<sub>2</sub> [1].

There are many methods to prepare TiO<sub>2</sub> photoelectrode, e.g. sol–gel [3,4], sputter deposition [11], anodic oxidation [12], etc. However, few works are reported to investigate the photocatalyst on titanium by direct thermal oxidation [7,13]. In this paper, we used the method to obtain photoelectrode in view of the following considerations: (a) complete formation of rutile TiO<sub>2</sub>; (b) it can obtain the optimal photoanode in view of light to electricity conversion efficiency compared to by anodic oxidation with subsequent reduction with hydrogen and by vapor deposition [14];

\* Corresponding author.

*E-mail address:* [lengwh@css.zju.edu.cn](mailto:lengwh@css.zju.edu.cn) (W.H. Leng).

and (c) to provide a reference for those photocatalysts formed on titanium metal substrate.

Aniline is commonly produced as by-product of the petroleum, coal and chemical industries. Due to its negative environmental impact there needs to develop methods to carry out its degradation. The studies of aromatic amines degradation have been examined by anatase  $\text{TiO}_2$  photocatalysis in suspension system [15,16]. The aim of this work was to investigate its photoelectrocatalysis behavior over rutile  $\text{TiO}_2$  electrode by using both double and single compartment photoreactors. The comparison of oxidation behavior of aniline in single and double compartment cell, and the role of oxygen were discussed simultaneously. The comparison between rutile and anatase  $\text{TiO}_2$  photoanode was preliminary investigated.

## 2. Experimental details

### 2.1. Materials

Titanium sheet (99.7%, in thickness 0.15 cm) was used for the preparation of photoanodes. Aniline was of analysis reagent and used as received, other chemicals and solvents were of reagent grade and used without further purification.  $\text{H}_2\text{SO}_4$  and/or  $\text{NaOH}$  adjusted the pH of solution before reaction. Double-distilled water was used throughout the work.

### 2.2. Photoanode preparation

Titanium sheet was cut into pieces  $12\text{ cm} \times 6\text{ cm}$  (sample A) and  $2\text{ cm} \times 2\text{ cm}$  (sample B), polished by  $1\text{ }\mu\text{m}$  diamond paper, chemically etched with an 3/1 (v/v) of  $\text{HNO}_3$  (68%)/ $\text{HF}$  for 15 s, and finally fully rinsed with double-distilled water, dried at room temperature. Samples were oxidized in furnace under an atmosphere of air as following: from room temperature increased to  $600\text{ }^\circ\text{C}$  at the rate of  $5\text{ }^\circ\text{C min}^{-1}$  and then hold at this temperature for 1 h, cooled to room temperature to obtain photoelectrodes. They were made an electrical contact by welding nickel wire on their backsides. The working area was 60 and  $3.9\text{ cm}^2$  for photoanode A and B, respectively, and the rest was covered with epoxy. Photoanode A and B were used for the photo-degradation of aniline and photoelectrochemical measurements, respectively.

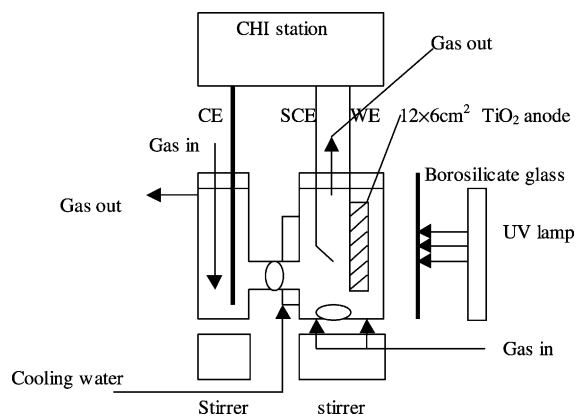


Fig. 1. Schematic diagram of photoelectrochemical reactor.

To obtain a  $\text{TiO}_2/\text{Ti}$  anatase film electrode, the titanium sheets (samples B) were dipped into  $\text{TiO}_2$  sol solutions for 30 s prepared by the method according to Tada and Honda [17], pulled up at the speed of  $2\text{ cm min}^{-1}$ , heated for 10 min at  $500\text{ }^\circ\text{C}$  to coat one layer, repeated this and the last coating heated for 1 h at  $500\text{ }^\circ\text{C}$ , then followed as above-mentioned procedures to obtain anatase photoanode (denoted as photoanode C).

### 2.3. Photoelectrochemical set-up

A H-type cell separated by a low porosity glass frit was used as shown in Fig. 1 (can be divided into two compartments). For double compartment cell, the anode compartment (solutions  $100\text{ cm}^3$ ) held the photoanode A (WE) and saturated calomel reference electrode (SCE), while the cathode compartment (solutions  $35\text{ cm}^3$ ) contained an Ag sheet counter electrode (CE). When conducted in a single compartment cell, all WE, CE and SCE were placed in above-mentioned anode compartment (solutions  $100\text{ cm}^3$ ). The initial concentration of aniline was  $10\text{ mg dm}^{-3}$  (including  $0.5\text{ mol dm}^{-3}$   $\text{Na}_2\text{SO}_4$  as supporting electrolyte) unless specified. All potentials in the text are versus SCE.

The presence or absence of oxygen in the anode and cathode compartment was controlled by purging oxygen/air or standard oxygen free nitrogen at a rate of  $16\text{ l h}^{-1}$  through pipettes with porosity glass frit prior to and during the experiments, respectively, and this is simplified in the form of anode:cathode, e.g.

N<sub>2</sub>:O<sub>2</sub>. The photoanode A was illuminated with a 4 × 6 W UV lamp ( $\lambda_{\max} = 365$  nm) filtered by borosilicate glass.

#### 2.4. Electroanalytical monitoring and potentiostatic control

For fixed potential experiments, the applied potential was kept constant in the dark for 30 s before illumination. Linear sweep voltammetry was carried out in a conventional borosilicate glass three-electrode cell. The working electrode was photoanode B, platinum spiral as the counter electrode, and SCE as the reference electrode. The light source was 6 W UV lamp. All experiments were carried out on CHI660 or Solartron 1280Z electrochemical station driven by a personal computer.

#### 2.5. Analyses

The aniline concentration in the solution was estimated colorimetrically (752 Spectrophotometer, Shanghai) [18]. NH<sub>4</sub><sup>+</sup> were estimated by phenate method [19]. The H<sub>2</sub>O<sub>2</sub> concentration was measured by the titration of KMnO<sub>4</sub> solution. The chemical oxygen demand (COD) was measured by coulometric titration of K<sub>2</sub>CrO<sub>7</sub> (HH-5 COD detector, Jianshu, China). The composition of photoanode on the surface was determined by X-ray photoelectron spectroscopy (XPS, VG Escalab MK II, Al K $\alpha$ , 15 kV–20 mA). The crystal structure of photoanode was measured by using X-ray diffractometer (XRD, Rigaku D/max-3B, Cu K $\alpha$ , 40 kV–40 mA, 0.2 °C min<sup>-1</sup>). The morphology of the film was determined by atomic force microscopy (AFM, AFM-II, Zhejiang University, China). The photons of the incident light inside the reactor in TiO<sub>2</sub>/Ti free solutions were measured employing potassium ferrioxalate actinometry [20] and evaluated to be  $2.38 \times 10^{-7}$  and  $2.53 \times 10^{-8}$  mol s<sup>-1</sup> for photoelectrochemical reactor and conventional three-electrode cell, respectively.

For detecting degradation products, organic solutions were analyzed by gas chromatography/mass spectrometry (GC/MS, HP 6890/5973) with a HP5 column (30 m × 0.25 mm). The oven was programmed as follows: isothermal at 45 °C for 2 min, from 45 to 250 °C at 6 °C min<sup>-1</sup>, and isothermal at 250 °C for 10 min. In the electron impact experiments, the elec-

tron energy was set at 70 eV and the electron current was set at 1 mA.

High-pressure liquid chromatograph (HPLC) was used (as an external standard method) to identify photoproducts (Spectra Physics 8810, C<sub>18</sub> column, UV detector working at 280 nm, CH<sub>3</sub>CN–water 60–40 vol.%, flow rate 0.7 ml min<sup>-1</sup>).

### 3. Results

#### 3.1. Characteristics of photoanode

XPS analysis shows that the surface composition of oxide film is TiO<sub>2</sub> (not shown here). This agrees to that direct thermally oxidation of titanium from 500 to 800 °C [13]. Fig. 2A shows the XRD spectra of photoanode. The principal peaks in the spectrum of TiO<sub>2</sub> are identified as the crystal of rutile form [13]. No anatase form was found in the specimens. Hartig et al. [14] have obtained the same results for TiO<sub>2</sub> formed thermally in air or oxygen atmosphere. The inset in Fig. 2A indicated the TiO<sub>2</sub> prepared by sol solution coating was the crystal of anatase form. The texture and morphology of photoanode can be observed in Fig. 2B. It shows that the surface is quite smooth and the particle size is less than 120 nm. The film thickness determined by a scanning electron microscope is ca. 250 nm.

#### 3.2. I–E relationship of TiO<sub>2</sub>/Ti electrode

Linear sweep voltammetry (LSV) was carried out on the photoanode B with 0.5 M Na<sub>2</sub>SO<sub>4</sub> as the supporting electrolyte. The starting potential was kept constant for 30 s and the potential was swept from –1.0 to +2.0 V at rate of 20 mV s<sup>-1</sup>. Fig. 3 shows the voltammograms recorded when oxygen was present or absent from the anodic compartment. Negligible current was found without irradiation (curve 1) through applying potential in a range from 0.0 to 2.0 V as shown in Fig. 3. On illumination of the TiO<sub>2</sub> electrode (curves 2–4), a significant increase in the anodic current was observed. The difference between the dark and light current gives the photocurrent. It is obvious that photocurrent increases with increasing the applied anodic bias potential.

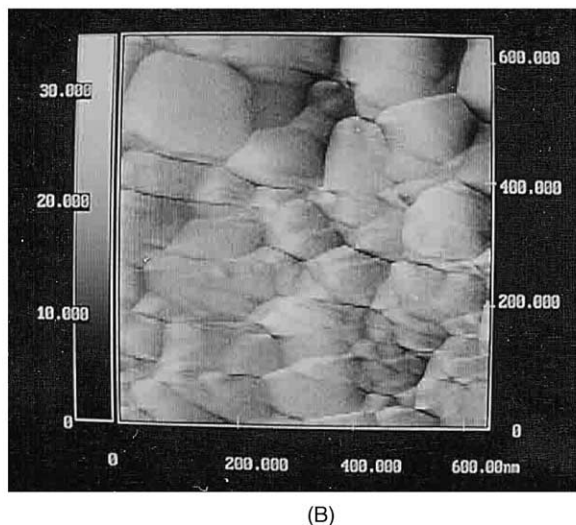
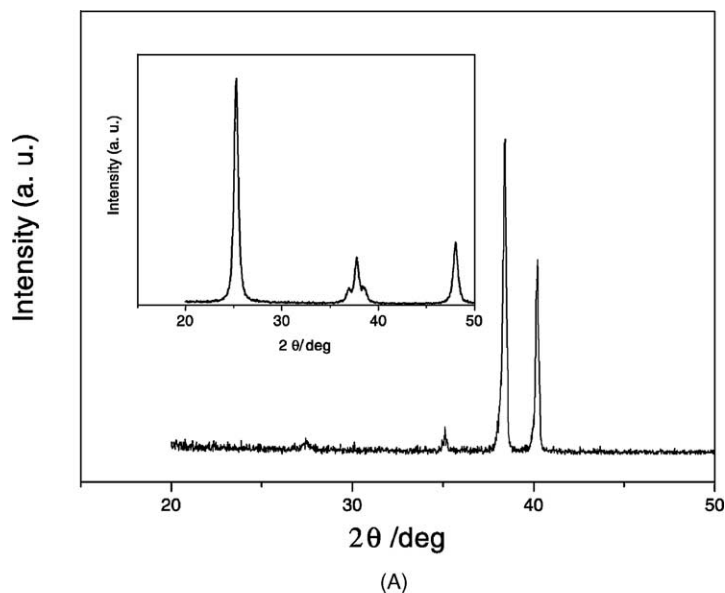


Fig. 2. (A) XRD pattern of  $\text{TiO}_2/\text{Ti}$  electrode (the inset shows the photoanode C). (B) AFM micrographs for  $\text{TiO}_2/\text{Ti}$  electrode.

When oxygen is present in anode compartment (curve 4), the photocurrent response is a little smaller than when oxygen is present in cathode alone (curve 3), but a slightly larger than when oxygen is absent from both compartments (curve 2). Also, the onset potential for anodic current is shifted more positives when oxygen is present in anode compartment than that with nitrogen (from  $-0.5$  to  $-0.36$  V). The quenching of anodic photocurrents due to the pres-

ence of oxygen in the anode, however, is not observed when positive potentials up to 0.5 V.

Fig. 4 presents LSV curves before and after the addition of aniline to the anode compartment. In the dark, there is no difference of anodic current between in the presence of aniline (Fig. 4, curve 1) and electrolyte alone (Fig. 3, curve 1). On illumination in the presence of rather low concentration of aniline, a slightly increase in the photocurrent is observed near

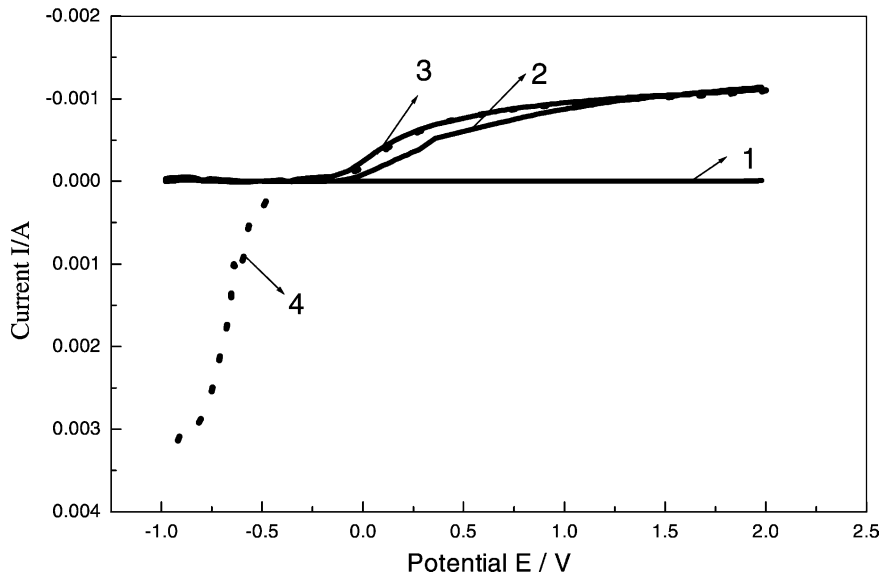


Fig. 3. Linear sweep voltammogram (LSV) for: (1) dark,  $\text{N}_2:\text{N}_2$ ; (2) light,  $\text{N}_2:\text{N}_2$ ; (3) light,  $\text{N}_2:\text{O}_2$ ; (4) light,  $\text{O}_2:\text{O}_2$ . Sweep rate =  $20 \text{ mV s}^{-1}$ , pH 6.70.

the onset potential of photocurrent with comparison to that without aniline in the anode compartment (Fig. 4, curves 6 and 7), but then the difference decreases with increasing positive potential. The photocurrent

decreases with increasing the concentration of aniline. Also the effect of gas on the photocurrent in the presence of aniline is similar to that with electrolyte only (see Fig. 3).

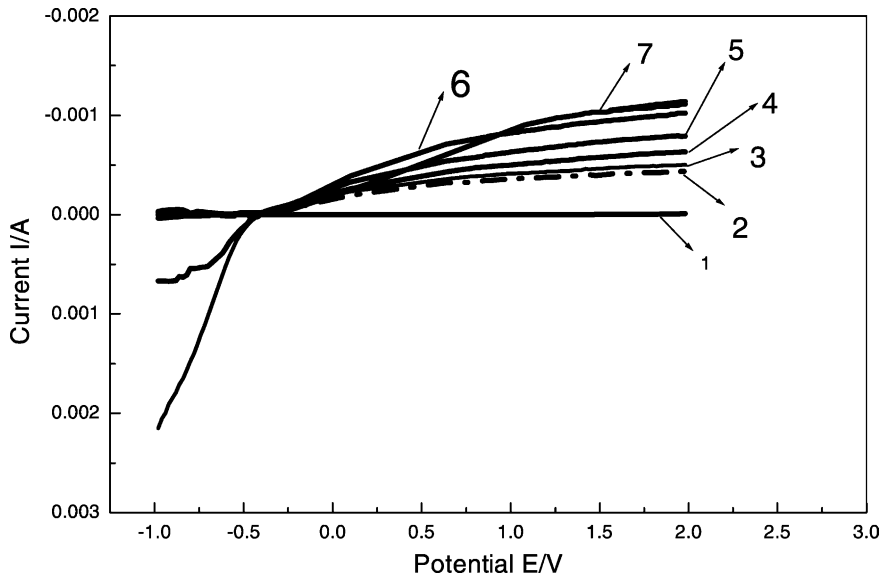


Fig. 4. Linear sweep voltammogram (LSV) for: (1) dark, aniline  $5 \times 10^{-4} \text{ M}$ ,  $\text{N}_2:\text{O}_2$ ; (2) light, aniline  $5 \times 10^{-3} \text{ M}$ ,  $\text{N}_2:\text{N}_2$ ; (3) light, aniline  $5 \times 10^{-3} \text{ M}$ ,  $\text{O}_2:\text{O}_2$ ; (4) light, aniline  $5 \times 10^{-3} \text{ M}$ , air: $\text{O}_2$ ; (5) light, aniline  $5 \times 10^{-3} \text{ M}$ ,  $\text{N}_2:\text{O}_2$ ; (6) light, aniline  $5 \times 10^{-4} \text{ M}$ ,  $\text{N}_2:\text{O}_2$ ; (7) light,  $0.5 \text{ M Na}_2\text{SO}_4$  only,  $\text{N}_2:\text{O}_2$ . Sweep rate =  $20 \text{ mV s}^{-1}$ , pH 6.70.

### 3.3. Comparison of photolysis, photocatalytic and photoelectrocatalytic degradation

As indicated in Fig. 5, a very small decrease in the concentration of aniline was observed both by electrochemical oxidation and photolysis for 1.5 h. The photocatalytic degradation of aniline was 13.8% for 1.5 h without applying potential (corresponding to open circuit). However, when applying anodic potential 1.0 V, the photo-degradation was increased to 61.7% with oxygen supply. Experimental results show that applying bias potential significantly increased the photo-oxidation rate of aniline and the oxidation reaction could occur even without oxygen as electron acceptor. It can also be seen that the rate was slower in N<sub>2</sub> saturated solutions (Fig. 5, curve 5) than that in O<sub>2</sub> (curve 4) in single compartment cell.

### 3.4. Influence of aniline concentration

Table 1 shows the independence of apparent first-order rate constants  $k_{app}$  and initial aniline concentrations both in single and double compartment cell. Obviously, the kinetics of aniline decay can be fitted in quasi-first-order reaction, the  $k_{app}$  decreases with increasing aniline concentration, and the rate in single compartment cell is larger than that in double compartment cell.

Table 1

Apparent first-order rate constants  $k_{app}$  and linear coefficient  $R^2$  for the photoelectrochemical degradation of aniline at different initial concentrations (experimental conditions: pH 6.70, applied potential +1.0 V, UV 1.5 h)

Concentration (mg dm <sup>-3</sup> )	Single compartment cell <sup>a</sup>		Double compartment cell <sup>b</sup>	
	$k_{app}$ (h <sup>-1</sup> )	$R^2$	$k_{app}$ (h <sup>-1</sup> )	$R^2$
5	0.6723	0.996	0.5523	0.991
10	0.3724	0.997	0.2817	0.98
15	0.2673	0.991	0.1591	0.995
20	0.201	0.995	0.1405	0.98
40	0.1396	0.998	–	–

<sup>a</sup> N<sub>2</sub> purged.

<sup>b</sup> Anodic:cathodic compartment = N<sub>2</sub>:O<sub>2</sub>.

### 3.5. Influence of applying bias potential

Experiments were carried out in N<sub>2</sub> or air saturated solutions both by single and double compartment cells. The effect of applied potential on the rate is shown in Fig. 6A. Increasing the applied potential from 0.0 to 2.0 V, the rate increased either by N<sub>2</sub> or air purging the solutions, but this becomes slowly when the potential up to 1.5 V. This is consistent with the photocurrent variation as shown in Figs. 3 and 4. It can also be observed that the rate with air is larger than that with N<sub>2</sub> by single compartment otherwise by double compartment cell. Also, the oxidation rate

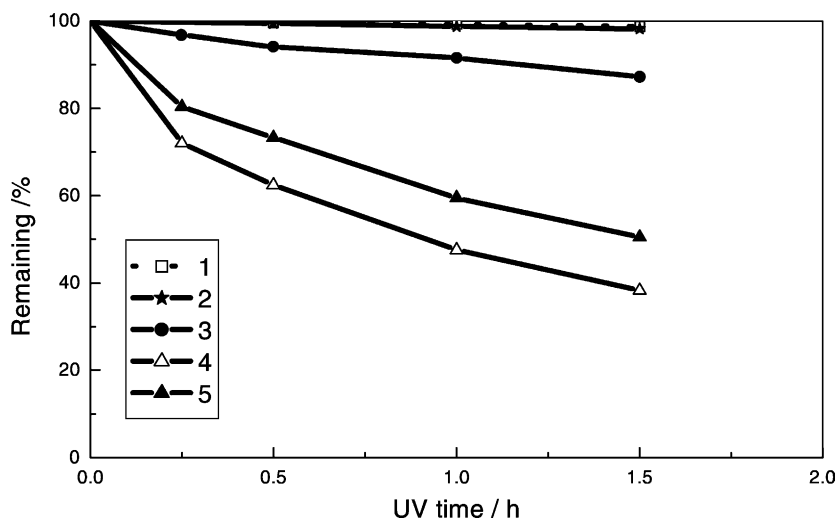


Fig. 5. Remaining of aniline against time for: (1) dark + O<sub>2</sub> + 1.0 V; (2) photolysis + O<sub>2</sub>; (3) photocatalysis + O<sub>2</sub>, no bias potential; (4) photocatalysis + O<sub>2</sub> + 1.0 V bias potential; (5) photocatalysis + N<sub>2</sub> + 1.0 V bias potential. Single compartment, pH 6.70.

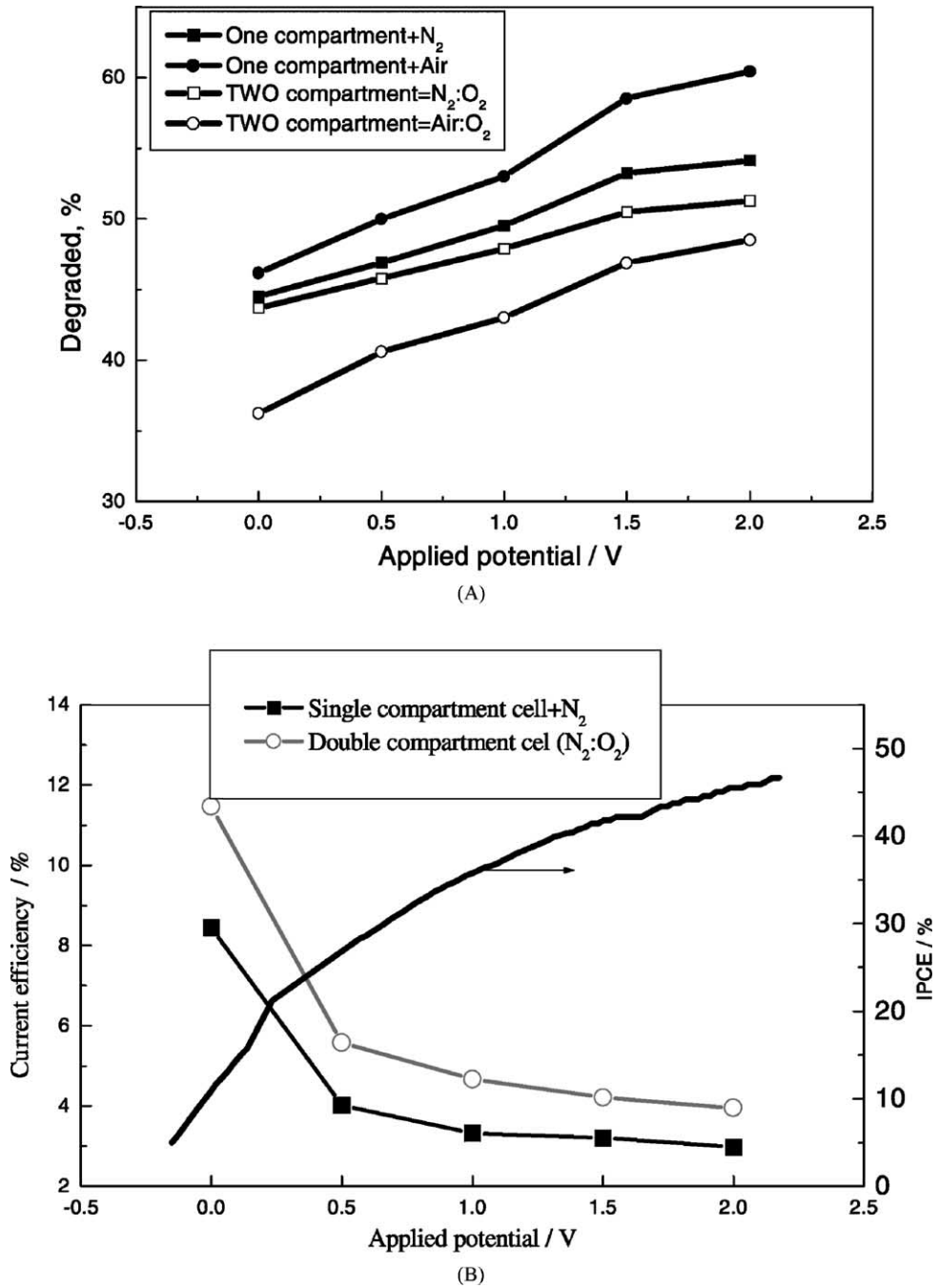


Fig. 6. Effect of applied potential on the aniline degradation rate (A) and on photocurrent efficiency of aniline photo-degradation (B) (pH 6.70; illumination 1.5 h).

in single compartment is larger than that in double compartment under the same gas atmosphere.

Suppose degrading 1 mol aniline to consume 1 mol photo-generating hole, then the photocurrent efficiency can be defined as:  $\eta = (\Delta cV)/(Q_t/F)$ , where

$\Delta c$  is the change of aniline concentration;  $V$  the solution volume,  $Q_t$  the passed charge,  $Q_t = \int_0^t I_{pH} dt$ ;  $F$  the Faraday's constant,  $F = 96,500 \text{ C mol}^{-1}$ . The incident photon to current efficiency (IPCE) is determined by the equation of  $\text{IPCE} = I_{pH}/[I_0F]$ , where

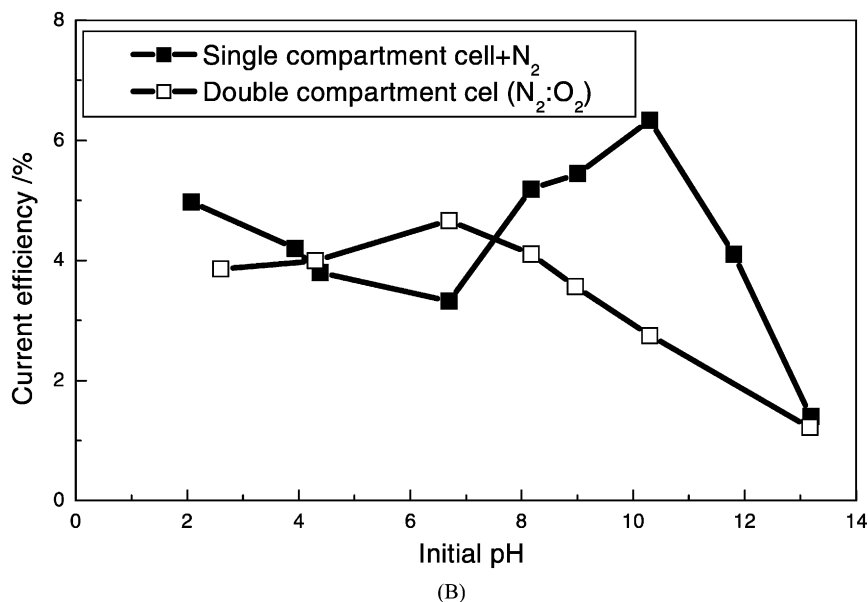
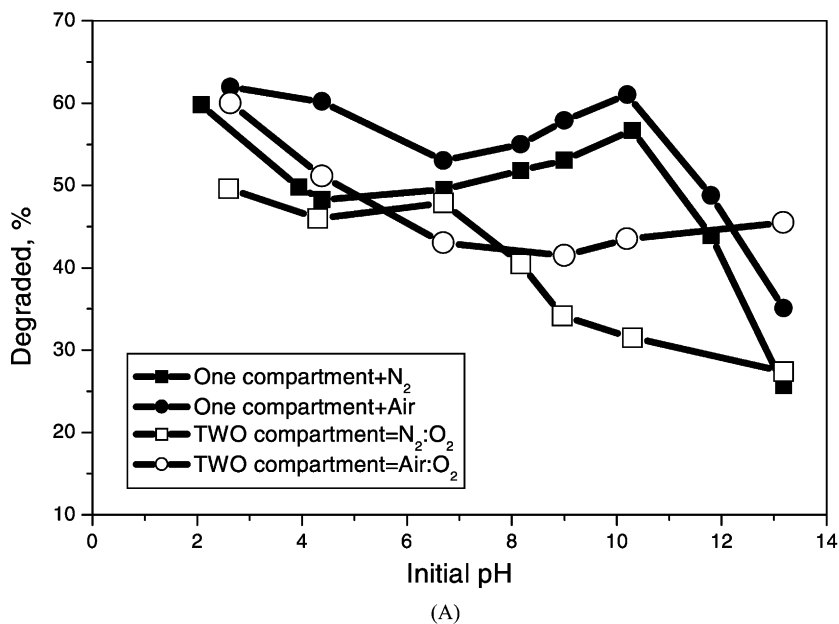


Fig. 7. Effect of pH on the aniline degradation rate (A) and on photocurrent efficiency of aniline photo-degradation (B) (bias potential 1.0 V; illumination 1.5 h).



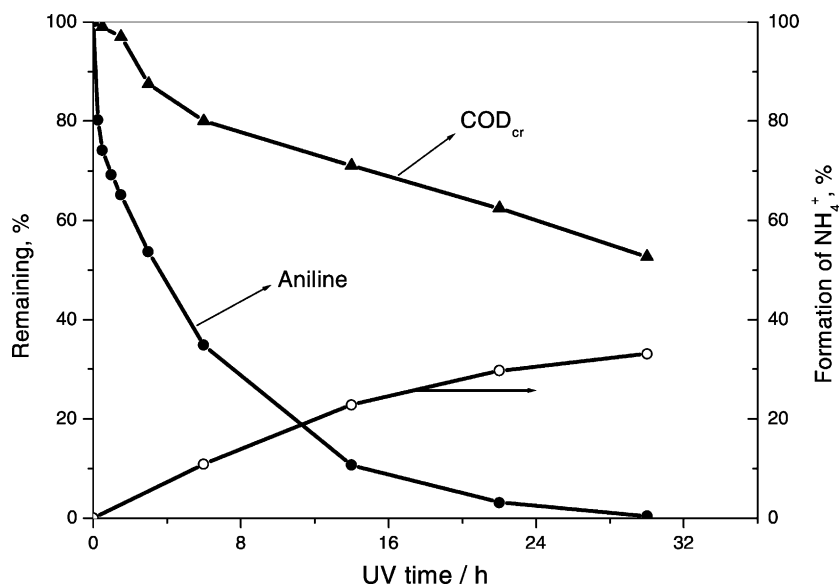


Fig. 8.  $\text{NH}_4^+$  formation, COD and aniline degradation (in double compartment cell,  $\text{O}_2:\text{O}_2$ ;  $C_0 = 20 \text{ mg dm}^{-3}$ , applied potential 1.0 V).

$I_{\text{pH}}$  and  $I_0$  are the photocurrent and incident light intensity, respectively. From Fig. 6B, it is found that  $\eta$  decreases quickly with increasing applied potential but becomes slowly when up to 1.0 V. However, the IPCE always increases quickly with increasing applied potential. Also the  $\eta$  in double compartment is larger than that in single compartment.

### 3.6. Influence of pH

For single compartment cell, increasing pH from 4.38 to 10.30, the rate increases, but when pH is larger than 10.30, it decreases sharply when purged with nitrogen as shown in Fig. 7A. It has the similar tendency when purged with air, but the rate of the former is smaller than that of the latter. For double compartment cell, the rate decreases with increasing pH without oxygen except in the range of pH 4–7. However, when with air in the anodic compartment, the rate decreases with increasing solution pH value. It can also be observed that the rate conducted in single compartment is larger than that in double compartment under the same gas atmosphere in anodic compartment.

For single compartment cell when purging with  $\text{N}_2$ ,  $\eta$  decreases with increasing pH in acid medium

while in alkaline  $\eta$  increases from pH 6.70 to pH 10.30, then decreases sharply when pH over 10.30 as shown in Fig. 7B. For double compartment cell (anode:cathode =  $\text{N}_2:\text{O}_2$ ),  $\eta$  decreases slowly whatever pH value higher or lower than 6.70.

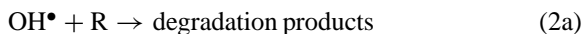
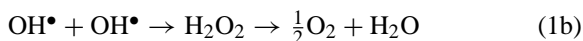
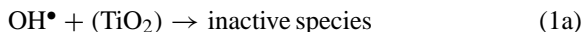
### 3.7. Degradation products

In order to determine whether the aniline was completely mineralized, photoelectrocatalytic degradation was conducted by double compartment cell in both compartments purging with pure oxygen. The variation of  $\text{NH}_4^+$ , COD and aniline was measured and the results were shown in Fig. 8. It shows that the aniline was completely disappeared while only 47.32% of COD removed when illuminated for 30 h. The COD decay was negligible for 1.5 h, and the complete mineralization of aniline took more time than its disappearance. Meanwhile only 33.14% of  $\text{NH}_4^+$  was formed. By analyzing the products, only one intermediate nitrobenzene was obtained in photoelectrocatalysis for 1.5 h both with or without oxygen in anodic compartment, detected by GC/MS (fragment  $m/e = 77, 65, 51$ ) and HPLC (nitrobenzene and intermediate product retention time was 6.66 and 6.7 min, respectively).

## 4. Discussion

### 4.1. Role of applied potential

Increasing anodic bias potential over TiO<sub>2</sub> photo-electrode leads to the increase of space charge layer and band bending, thus promotes the separation of photo-generating carriers and interface charge transfer rate of semiconductor/solution, causes to increase the photocurrent and quantity of active species, consequently, the rate increases. However, the thickness of space charge layer cannot be larger than the film thickness, and also the photo-carriers are separated fully under high enough bias potential (for given light intensity), thus cause saturated photocurrent and the rate increases slowly. Inversely, photocurrent efficiency decreases with increasing bias potential as indicated in Fig. 6B. This is hard to explain, possible reason is the rate of Eq. (1) increasing more than that of Eq. (2).



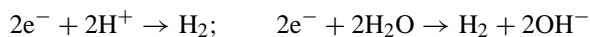
### 4.2. Role of oxygen

Since the influence of applied potential, solution pH and solute concentration on the rate has been examined fully, here we will emphasis the comparison of photoelectrocatalytic behavior of aniline in single and double compartment cell, and the role of oxygen is considered simultaneously.

Oxygen is the usual electron acceptor for photocatalysis. Adsorbed oxygen scavenges conduction band electrons from the TiO<sub>2</sub> surface preventing them from reaching the supported substrates, so the reduction in the anodic current in the presence of oxygen was observed as shown in Figs. 3 and 4. This quenching of anodic photocurrent near the onset potential for photocurrent, however, was not observed at positive potentials up to 0.5 V, which indicates the charge separation is efficient in TiO<sub>2</sub> film when the applied potential up to 0.5 V.

Oxygen is crucial to photocatalytic reactions in open circuit system. The reduction of oxygen might

become rate limiting under a certain condition [21]. Photo-oxidation under open circuit cannot occur in the presence of nitrogen saturate solutions and without anodic bias potential, which indicates the photo-carriers have recombined. However, with a certain anodic bias potential, the photoproducing electrons are moved to the counter electrode where the following reaction can occur even without oxygen. So the photo-oxidation reaction can be occurred.



Since the standard reduction potential of oxygen is more negative than that of the above two reaction, which suggests the former is favorable to proceed, thus the photocurrent with oxygen in cathode compartment was larger than that without oxygen as indicated in Figs. 3 and 4. This also means there leave more separated photogenerating holes because the electron has been removed by oxygen. The products of oxygen reduction, e.g. HO<sub>2</sub><sup>-</sup> and H<sub>2</sub>O<sub>2</sub> can also react with organic compound of interest. To confirm this, the accumulative concentration of H<sub>2</sub>O<sub>2</sub> in cathode compartment was measured and evaluated to be 12.74 mM after passing electric charge 123 C (pH 12.8, applied potential 0.0 V, light intensity 8.05 × 10<sup>-7</sup> mol s<sup>-1</sup>, 35 cm<sup>2</sup> graphite cathode with oxygen purging). However, H<sub>2</sub>O<sub>2</sub> cannot easily be detected on Ag cathode because oxygen may be four-electron reaction (producing less H<sub>2</sub>O<sub>2</sub>) and/or H<sub>2</sub>O<sub>2</sub> can be catalytically decomposed on it. Fig. 9 shows the degradation of aniline in cathode compartment when using double compartment cell, which means that the products of oxygen reduction can oxidize aniline. In addition, oxygen acts as oxidant in the process of the hydroxylation of organic substance [4,22]. So the oxidation rate of aniline with oxygen was larger than without oxygen for single compartment cell as indicated in Fig. 5A or 6A, though smaller the photocurrent of the former was. This can also account for the case of using double compartment cell except near the neutral pH as indicated Fig. 6A or 7A.

But why are the rates in single compartment cell larger than in double compartment cell under the same gas atmosphere?

The photoanode reactions (e.g. consuming OH<sup>-</sup> or produce H<sup>+</sup>) usually cause the solution pH to decrease, while the cathode reactions (e.g. consuming H<sup>+</sup>) do increase the pH. So the solution pH should not

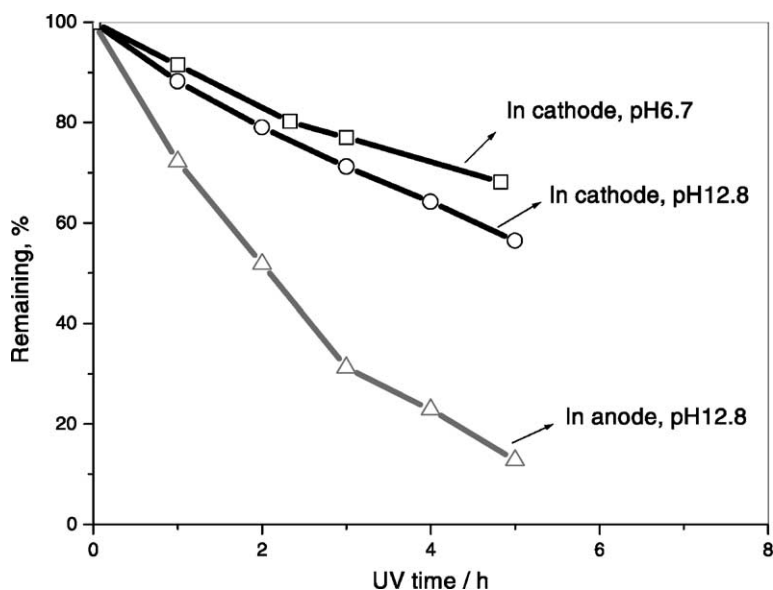
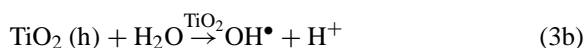
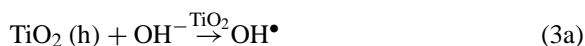


Fig. 9. Removal rate of aniline in both compartment cells (anode  $N_2$  purged,  $C_0 = 10 \text{ mg dm}^{-3}$ ; cathode  $O_2$  purged  $C_0 = 5 \text{ mg dm}^{-3}$ ; applied potential 0.0 V).

change too much when photoelectrocatalytic degradation of aniline conducted in single compartment cell. This is confirmed by the results as indicated in Fig. 10A. However, when performed in double compartment cell, the anodic and cathode reaction occur at different sites, thus it causes pH in the anode compartment to decrease and increase in the cathode compartment as shown in Fig. 10. The pH decreasing largely in anodic compartment may hinder the reaction (3) proceed. Similarly, the pH increasing largely in the cathode compartment may impede some reduction reactions (e.g.  $H^+$  or  $H_2O$  reduction). All above may contribute to that the rates of aniline in double compartment cell was lower than that in single compartment cell under the same gas purging.



Question may arise that the photoproducts may change the solution pH. However, it was found there had the same pH variations with  $Na_2SO_4$  alone in water. In addition, as above mentioned that the COD change was negligible and intermediate products ni-

trobenzene cannot make pH change so much. So, we need not consider it.

Based on above results, we deem it was the pH variations in both compartments that arose the rates in single compartment cell larger than in double compartment cell under the same gas atmosphere.

Aniline can be mineralized completely by photocatalysis [15,16]. For OH radical mediated degradation of aniline Brillas et al. [19] have proposed two different pathways: (a) through hydrogen abstraction and formation of an imino radical, which can release  $NH_4^+$ ; (b) through the oxidation to nitrobenzene. In the experiments the detection of nitrobenzene and  $NH_4^+$  is consistent with their proposed mechanism. This means that  $NH_4^+$  is not the sole transformation of organic nitrogen, which can be proved in Fig. 8 that nitrogen mass was out of balance.

#### 4.3. Comparison with anatase $TiO_2$ photoanode

Finally, further remarks are that the photocurrent of anatase  $TiO_2/Ti$  electrode was prone to saturate while the rutile one did not in the range of applied potential from 0.0 to +1.0 V though the former was larger than the latter as indicated in Fig. 11. When the

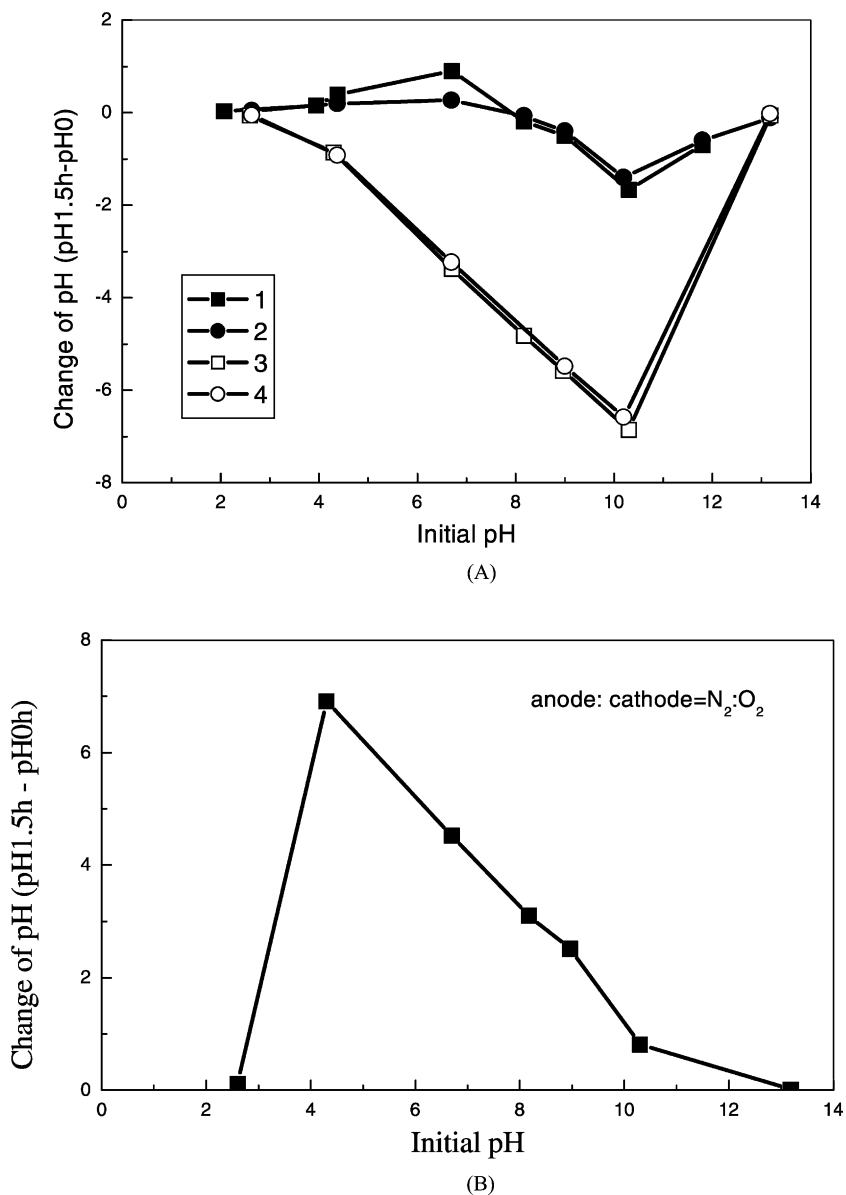


Fig. 10. Variation of pH in anode compartment (A) and cathode compartment (B) against the initial pH for aniline degradation 1.5h (experimental conditions same to Fig. 7). Single compartment: 1, N<sub>2</sub> purged; 2, air purged. Double compartment: 3, N<sub>2</sub>:O<sub>2</sub>; 4, air:O<sub>2</sub>.

photocurrent is saturate the rate may no longer improve, e.g. Kim and Anderson [9] reported that increasing the positive potential above 0.0 V on anatase TiO<sub>2</sub> form electrode had no effect on the rate of oxidation of formic acid. It seems here that the oxidation rate on rutile TiO<sub>2</sub>/Ti electrode can be im-

proved by exerting more broader range of anodic potential.

We have also made a preliminary comparison of the above two types of TiO<sub>2</sub>, i.e. photoanode B and C (coating six layers) in terms of the oxidation rate of aniline (photoactivity) at an applied potential 0.5 V, pH

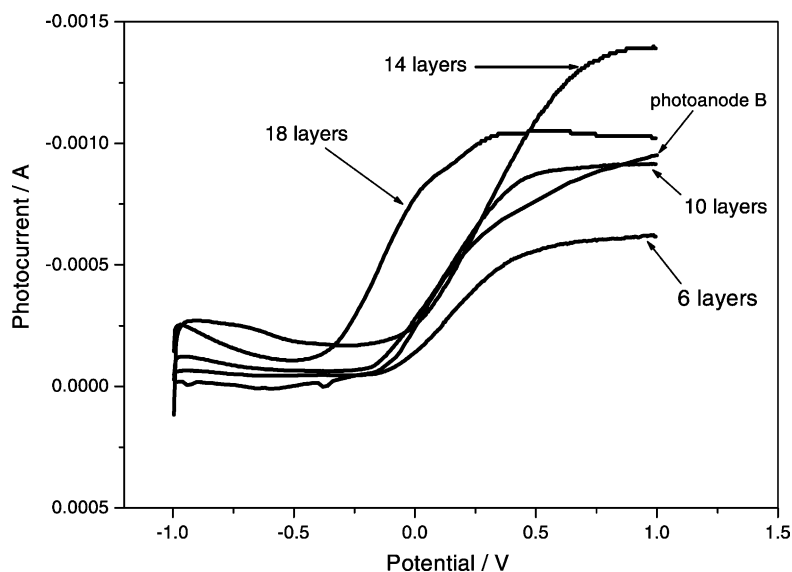


Fig. 11. Comparison of photocurrent on anatase and rutile  $\text{TiO}_2/\text{Ti}$  electrodes (light,  $\text{N}_2:\text{O}_2$ ; sweep rate =  $20 \text{ mV s}^{-1}$ , pH 6.70).

6.70. The results (not shown here) indicated that the photocurrent efficiency  $\eta$  is lower for rutile, though the rutile electrode gave a higher IPCE than the anatase electrode as indicated in Fig. 11. So the total result is the quantum yield  $\Phi$  ( $\Phi = \eta \times \text{IPCE}$ ) for rutile slightly higher than for the anatase electrode. This may be attributed to a part of the photocurrent is used for water oxidation in the case of rutile electrode. Detail differences and their reasons between rutile and anatase need further investigation, and this is under way in our laboratory.

## 5. Conclusions

The photocatalytic oxidation of aniline in a  $\text{Na}_2\text{SO}_4$  solution could be electrochemically promoted by applying bias potential on the rutile form of a  $\text{TiO}_2$  film electrode prepared by direct thermally oxidation of titanium. No oxygen supply was required in photoelectrocatalytic degradation of aniline, but oxygen and its reduction products could accelerate the oxidation rate of aniline. The rate performed in single compartment cell was larger than in double compartment cell with air/nitrogen purging the anodic compartment. The photocurrent reflected the oxidation rate of aniline but

it was dependent on oxygen and the photocurrent efficiency was related to potential, pH, and single/double compartment cell.

## Acknowledgements

A part of the work was Financial support from the Foundation of National Science Council, China (Grant 20107006).

## References

- [1] M.R. Hoffman, S.T. Martin, W. Choi, et al., *Chem. Rev.* 19 (1995) 69.
- [2] R.J. Candal, W.A. Zeltner, M.A. Anderson, *Environ. Sci. Technol.* 34 (2000) 3443.
- [3] K. Vinodgopal, S. Hotchandani, P.V. Kamat, *J. Phys. Chem.* 97 (1993) 9040.
- [4] K. Vinodgopal, U. Stafford, K.A. Gray, et al., *J. Phys. Chem.* 98 (1994) 6797.
- [5] J.M. Kesselman, G.A. Shreve, M.R. Hoffman, et al., *J. Phys. Chem.* 98 (1994) 13385.
- [6] H. Hidaka, T. Shimura, K. Ajisaka, et al., *J. Photochem. Photobiol. A: Chem.* 109 (1997) 165.
- [7] S. Chih-Cheng, C. Tse-chuan, *Ind. Eng. Chem. Res.* 37 (1998) 4207.
- [8] H. Hidaka, K. Ajisaka, S. Horikoshi, et al., *Catal. Lett.* 60 (1999) 95.

- [9] D.H. Kim, A. Anderson, *Environ. Sci. Technol.* 28 (1994) 479.
- [10] S. Chih-Cheng, C. Tse-chuan, *J. Mol. Catal. A: Chem.* 151 (2000) 133.
- [11] J. Rodríguez, M. Gómez, S.-E. Lindquist, et al., *Thin Solid Films* 360 (2000) 250.
- [12] J.A. Byrne, B.R. Eggins, N.M.D. Brown, et al., *Appl. Catal. B: Environ.* 17 (1998) 25.
- [13] R. Palombari, M. Ranchella, C. Rol, et al., *Sol. Energy Mater. Sol. Cells* 71 (2002) 359.
- [14] K.J. Hartig, N. Getoff, G. Nauer, *Int. J. Hydrogen Energy* 8 (1983) 603.
- [15] E. Pramauro, A.B. Prevot, *Analyst* 120 (1995) 237.
- [16] L. Sánchez, J. Peral, X. Domènech, *Electrochim. Acta* 42 (1997) 1877.
- [17] H. Tada, H. Honda, *J. Electrochem. Soc.* 142 (1995) 3438.
- [18] L. Wenhua, Liuhong, C. Shao'an, et al., *J. Photochem. Photobiol. A: Chem.* 131 (2000) 125.
- [19] E. Brillas, R.M. Bastida, E. Uosa, *J. Electrochem. Soc.* 142 (1995) 1733.
- [20] A.L. Pruden, D.F. Ollis, *J. Catal.* 82 (1983) 404.
- [21] H. Gerischer, A. Heller, *J. Phys. Chem.* 95 (1991) 5261.
- [22] K.-i. Okamoto, Y. Yamamoto, H. Tanaka, A. Itaya, *Bull. Chem. Soc. Jpn.* 58 (1985) 2015.